



Dramatic response of metastatic cutaneous angiosarcoma to an immune checkpoint inhibitor in a patient with xeroderma pigmentosum: whole-genome sequencing aids treatment decision in end-stage disease

Sophie Momen,^{1,2} Hiva Fassihi,² Helen R. Davies,^{1,3} Christos Nikolaou,⁴ Andrea Degasperi,^{1,3} Catherine M. Stefanato,⁵ Joao M. L. Dias,^{1,3} Dhruva Dasgupta,⁶ Emma Craythorne,² Robert Sarkany,² Sophie Papa,^{4,7} and Serena Nik-Zainal^{1,3}

¹Department of Medical Genetics, Addenbrooke's Treatment Centre, The Clinical School, University of Cambridge, Cambridge Biomedical Campus, Cambridge CB2 0QQ, United Kingdom; ²National Xeroderma Pigmentosum Service, Department of Photodermatology, St John's Institute of Dermatology, Guy's and St Thomas' Foundation Trust, London SE1 7EH, United Kingdom; ³MRC Cancer Unit, Hutchison/MRC Research Centre, University of Cambridge, Cambridge Biomedical Campus, Cambridge CB2 0XZ, United Kingdom; ⁴Department of Medical Oncology, Guy's and St Thomas' NHS Foundation Trust, Great Maze Pond, London SE1 9RT, United Kingdom; ⁵Department of Dermatopathology, St John's Institute of Dermatology, Guy's and St Thomas' Foundation Trust, London SE1 7EH, United Kingdom; ⁶Department of Nuclear Medicine, Guy's and St Thomas' NHS Foundation Trust, Great Maze Pond, London SE1 9RT, United Kingdom; ⁷School of Cancer and Pharmaceutical Studies, King's College London, Guy's Campus, Great Maze Pond, London SE1 9RT, United Kingdom

Corresponding author:
sophie.momen@doctors.org.uk

© 2019 Momen et al. This article is distributed under the terms of the Creative Commons Attribution License, which permits unrestricted reuse and redistribution provided that the original author and source are credited.

Ontology term: metastatic angiosarcoma

Published by Cold Spring Harbor Laboratory Press

doi:10.1101/mcs.a004408

Abstract “Mutational signatures” are patterns of mutations that report DNA damage and subsequent repair processes that have occurred. Whole-genome sequencing (WGS) can provide additional information to standard diagnostic techniques and can identify therapeutic targets. A 32-yr-old male with xeroderma pigmentosum developed metastatic angiosarcoma that was unresponsive to three lines of conventional sarcoma therapies. WGS was performed on his primary cancer revealing a hypermutated tumor, including clonal ultraviolet radiation-induced mutational patterns (Signature 7) and subclonal signatures of mutated DNA polymerase epsilon (*POLE*) (Signature 10). These signatures are associated with response to immune checkpoint blockade. Immunohistochemistry confirmed high PD-L1 expression in metastatic deposits. The anti-PD-1 monoclonal antibody pembrolizumab was commenced off-label given the *POLE* mutation and high mutational load. After four cycles, there was a significant reduction in his disease with almost complete resolution of the metastatic deposits. This case highlights the importance of WGS in the analysis, interpretation, and treatment of cancers. We anticipate that as WGS becomes integral to the cancer diagnostic pathway, treatments will be stratified to the individual based on their unique genomic and/or transcriptomic profile, enhancing classical approaches of histologically driven treatment decisions.

INTRODUCTION

Xeroderma pigmentosum (XP) is a rare, autosomal recessive disorder of nucleotide excision repair (NER), with an incidence in Western Europe of 2–3 per million live births (Kleijer et al. 2008). There are eight different complementation groups, dependent on the XP protein that is mutated (XP-A through G and V). The XP-A to G proteins are involved in repairing bulky DNA damage caused by ultraviolet radiation (UVR)—namely, cyclobutane pyrimidine dimers (CPDs) and 6–4 pyrimidine-pyrimidone photoproducts (Brash 2015). Unrepaired CPDs cause a UVR-related mutational signature characterized by C > T and CC > TT substitutions (Brash 2015). As a result of the excess of UVR-related damage, patients develop exposed-site pigmented changes, multiple skin cancers, and ocular surface disease and one-third of patients develop progressive neurodegeneration (Fassihi et al. 2016). XP patients have a 2000-fold increased incidence of melanoma, and a 10,000-fold increased incidence of non-melanoma skin cancer (Bradford et al. 2011).

The immune system plays a critical role in the surveillance of malignant cells. However, its effectiveness can be restricted by various immune-escape or checkpoint mechanisms. In particular, the programmed death protein (PD-1) binds to ligands PD-L1 and PD-L2. Upon activation, T cells express PD-1, which interacts with PD-L1 on tumor and stromal cells, deactivating the T cells and negatively regulating T-cell effector functions (Gentzler et al. 2016).

Immune checkpoint inhibitors interfere with these checkpoints, reactivating antitumor activity of cytotoxic T cells. Immunotherapies like anti-PD-1 and anti-PD-L1 have revolutionized the treatment of certain malignancies, especially melanoma (Gentzler et al. 2016). Their role in treating other solid organ malignancies is expanding (Gentzler et al. 2016). Higher tumor PD-L1 levels may be an indicator of an enhanced response to treatment. However, the role of PD-L1 as a predictive biomarker is controversial, as there is a subset of PD-L1 negative tumors that still respond to PD-1/PD-L1 inhibition (Gentzler et al. 2016). Tumors with high mutational loads have been shown to demonstrate a greater response to immune checkpoint blockade (Howitt et al. 2015). One explanation for this is the creation of a large number of neoantigens. Nevertheless, other factors are likely to play a role, as not all hypermutated tumors respond in the same way (Howitt et al. 2015).

Somatic mutations in the proofreading exonuclease domain of DNA polymerase epsilon (*POLE*) have been associated with tumors of high mutational loads (Shinbrot et al. 2014). Mutations in *POLE* have been reported in colorectal and 10% of endometrial cancers (Gargiulo et al. 2016). In a study of hypermutated endometrial cancers ($>232 \times 10^{-6}$ mutations/Mb), tumors with somatic *POLE* mutations were associated with a 15-fold higher number of neoepitopes per sample when compared to tumors with microsatellite instability (MSI). *POLE*-mutated and MSI tumors also had a higher number of CD3⁺ ($P=0.001$) and CD8⁺ ($P<0.001$) tumor-infiltrating lymphocytes (TILs) compared to microsatellite-stable tumors. *POLE* mutations are associated with increased PD-1 and PD-L1 expression (Howitt et al. 2015). PD-1 was shown to be overexpressed in TILs and peritumoral lymphocytes of *POLE*-mutated tumors, thus suggesting that *POLE*-mutated tumors may be candidates for PD-1/PD-L1-targeted immunotherapies (Howitt et al. 2015). *POLE* mutations have been demonstrated in an extensive number of tumor types that have shown sensitivity to checkpoint inhibitors (Gargiulo et al. 2016).

RESULTS

Case

A 32-yr-old Caucasian male with XP complementation group C (compound heterozygous mutations; c.445_446delGA in exon 4a and c.2336 del T in exon 13 in *XPC*) (XP1SH)



Figure 1. Clinical image of patient highlighting angiosarcoma on the medial aspect of his left eyebrow.

presented in January 2017 with a rapidly growing violaceous nodule on the left supraorbital area (Fig. 1). He had a history of multiple non-melanoma skin cancers. Histopathology demonstrated a dense dermal infiltrate of pale, eosinophilic, neoplastic cells extending from the papillary to the reticular dermis. These cells “dissected the collagen bundles” and had enlarged and hyperchromatic nuclei (Fig. 2A,B). Immunostaining was positive for vascular markers CD31 and ERG (Fig. 2C,D). The neoplastic cells were negative for S100, CD34, and MFT 116. All these findings were in keeping with the diagnosis of cutaneous angiosarcoma. Positron emission tomography–computed tomography (PET-CT) showed no metastatic disease. A wide local excision was undertaken at the regional sarcoma unit, and clear margins were reported. Adjuvant radiotherapy was not given. Eight months later, he presented with a right submandibular palpable mass; fine-needle aspiration confirmed metastatic angiosarcoma. A repeat PET-CT showed bilateral submandibular nodes. He was commenced on ifosfamide and doxorubicin at a standard dosing, which was well-tolerated. After six cycles, a PET-CT showed metastatic disease in the lung and liver. Eighteen months after diagnosis he was enrolled into the TAPPAS trial of TRC105 (carotuximab, a monoclonal antibody targeting CD105) and pazopanib versus pazopanib alone. After 1 month there was suspicion of clinical disease progression, and upon repeat imaging, further metastatic disease was confirmed, with mediastinal, pericardial, pleural, liver, and bony infiltration (Fig. 3). A base-of-skull metastasis demonstrated direct cranial extension. His Eastern Collaborative Oncology Group-Performance Status (ECOG-PS) was 3 and he was admitted as an inpatient with severe cachexia, anorexia, and concerns about imminent terminal complications of his disease. Bilateral pneumothoraces were treated with video-assisted thoracic surgery (VATS) procedures and pleurodeses. Palliative radiotherapy 36 Gy in 12 fractions was given to a mandibular tumor deposit because of impending tracheal compression (Fig. 4). WGS was performed on a primary tumor biopsy (Fig. 5).

Genomic Analysis

Driver mutations were identified in *TP53* (H179Y, variant allele fraction of 26%) and *CDKN2A* (homozygous whole-gene deletion). Driver mutations linked to angiogenesis previously

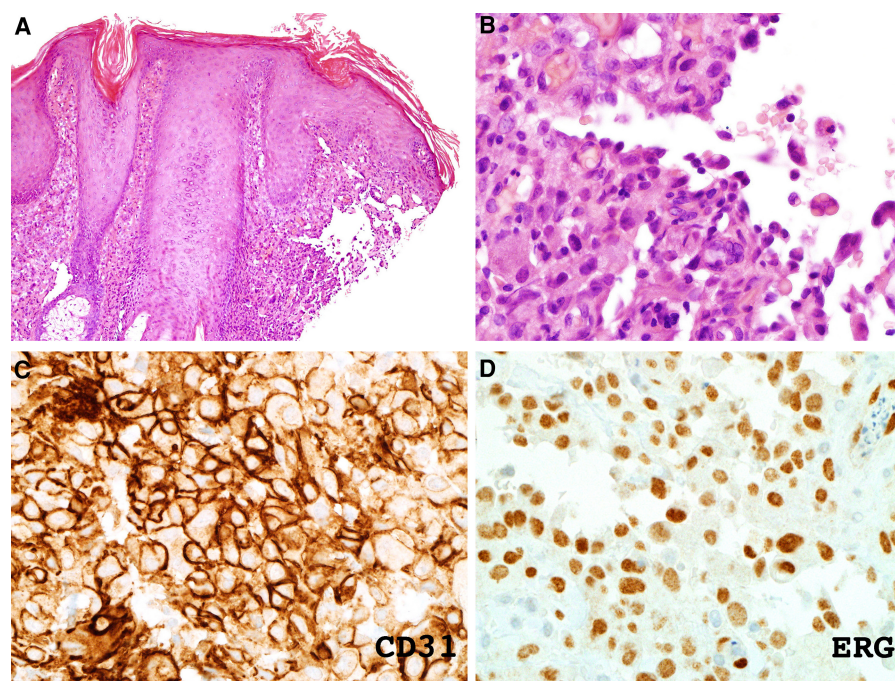


Figure 2. (A,B) Hematoxylin and eosin staining of skin biopsy shows dermal infiltrate of pale eosinophilic cells that have characteristic features of “dissecting the collagen bundles” and atypical, enlarged, and hyperchromatic nuclei. (C,D) Immunostaining shows staining for vascular markers CD31 and ERG (labeled).

reported in angiosarcomas, *PTPRB* and *PLCG1*, were not observed (Behjati et al. 2014). Mutations in *TP53* and homozygous deletions of *CDKN2A* have previously been reported in angiosarcomas (Behjati et al. 2014). WGS additionally revealed an extremely high mutational load of 805,261 substitutions and 1007 small insertions/deletions (indels) (Fig. 5). Two base substitution mutational signatures were identified. Signature 7, the classic “UV signature” (Alexandrov et al. 2013) comprising C > T transitions and CC > TT double substitutions accounted for 91.2% of these. This is the mutational signature that is commonly seen in melanoma (Pleasant et al. 2010). In a patient with deficient NER, this signature would be expected, even in noncancerous “normal” skin. However, Signature 10 was also identified, accounting for a small fraction of 8.8% of the mutational load in the primary tumor. This signature is characterized by three distinctive substitution peaks—C > A substitutions at TCT trinucleotides, C > T substitutions at TCG trinucleotides and T > G substitutions at TTT trinucleotides—and is reported in association with activating driver mutations in the proofreading exonuclease domain of *POLE* (Cancer Genome Atlas Network 2012). The possibility that this mutation was present in a subclone of the primary tumor was raised. Closer inspection revealed a subclonal driver mutation in *POLE* (S459F, variant allele fraction of 17%). Although it is a noncanonical *POLE* mutation, it maps to the Exo III motif of the endonuclease. Functional work supports reduced proofreading activity of an expression construct carrying this mutation, supporting driver potential, and it is this mutation that was driving the patient’s metastatic disease (Shinbrot et al. 2014).

Both a high mutational burden and somatic mutations in *POLE* are reported to be predictors of sensitivity to immune checkpoint inhibitors. Consistent with this prediction, immunohistochemistry of PD-L1 was positive on both the primary excision and on a metastatic lymph node deposit (60% positivity) (Fig. 6). However, anti-PD-/PD-L1 therapy for angiosarcoma is not currently licensed given the lack of clinical trial data supporting its use (Table 1).



Figure 3. Figure showing response of disease after four cycles of pembrolizumab. Pretreatment CT image (*left*) and PET-CT scan after four cycles of pembrolizumab (*right*). The *top* row shows a reduction in the size of liver metastases; the *middle* row shows a reduction in the size of lung metastatic deposits; and the *bottom* row shows the mediastinal response.

Treatment Outcomes

The anti-PD-1 monoclonal antibody pembrolizumab at 200 mg every 3 weeks was commenced off-label given the *POLE* mutation and high mutational load. Treatment was tolerated well with no side effects. After four cycles there was evidence of resolution of the lung and bone disease and almost complete resolution of the cardiac disease and pericardial effusions. There was significant reduction in the liver metastases and the residual visible liver disease was no longer FDG-avid (Fig. 3). Activity remained in a soft tissue jaw mass and pleural tissue; however, these were significantly reduced in volume (Fig. 4). The remaining jaw uptake is suggestive of osteoradionecrosis and may not represent ongoing malignant disease. His weight has increased from 48 kg to 56 kg and ECOG-PS is 0. Diuretics, high dose steroids, and opiates have been weaned completely. He has now had 11 cycles, he is back at work full-time, and treatment is ongoing.

DISCUSSION

Angiosarcoma and XP

Cutaneous angiosarcomas are rare malignancies of endothelial cells that often occur on the head and neck of the elderly (Griffiths et al. 1998). They arise spontaneously or secondary to ionizing radiation or chronic lymphoedema (Griffiths et al. 1998). Angiosarcoma has a poor

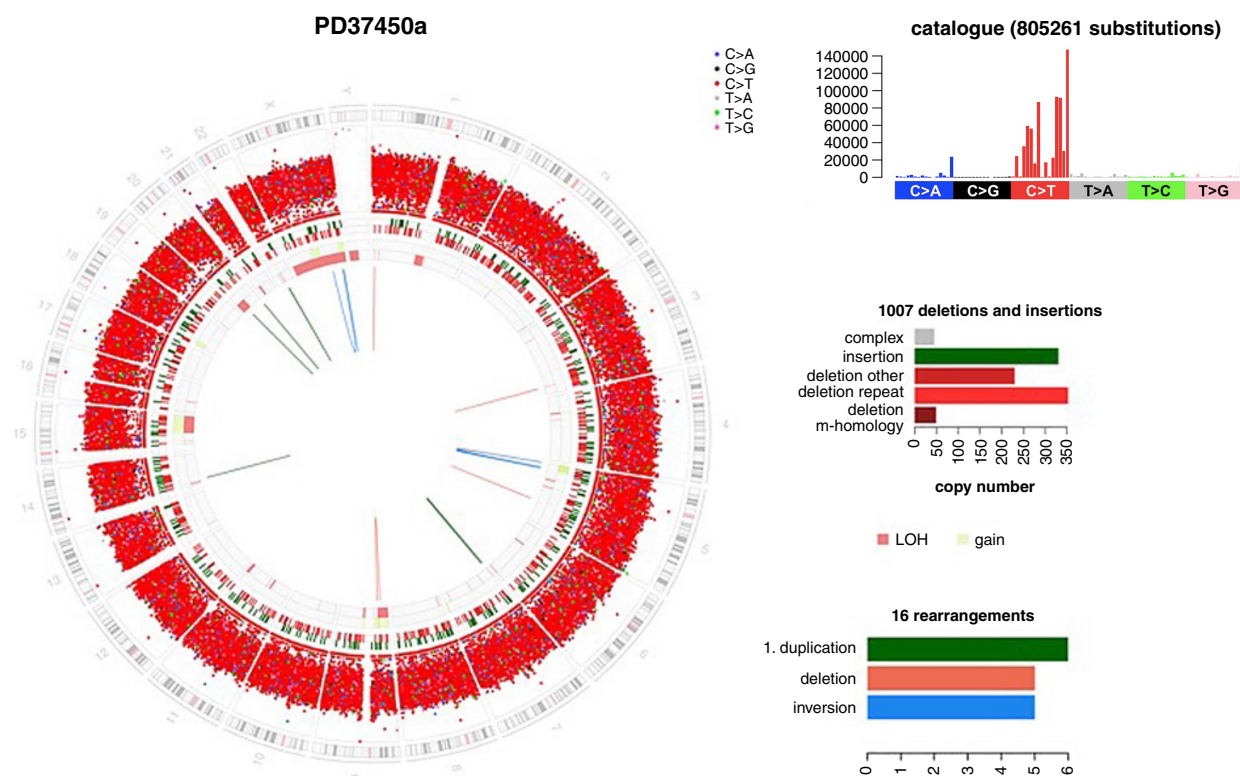


Figure 4. Circos plot of whole-genome sequenced angiosarcoma. It depicts a chromosomal ideogram on the outermost ring. Moving inward, the next ring shows a large number of C > T transitions. The next ring depicts small (<100-bp) insertions (green) and deletions (red). Then the next rings report copy-number state (green = gains, pink = losses), and the lines in the center of the plot report structural variants, of which there are not many. The *right-hand top* panel displays the substitution mutation profile. This graph shows that there are 805,261 C > T transitions with a mutational profile that is typical of UV damage. The *right-hand middle* panel shows the distribution of classes of indels, of which there are 1007. The *right-hand bottom* panel shows the types of structural variants that are present in this tumor.

prognosis, and metastatic disease is common. It has an estimated mean 5-yr survival rate of 33.5% (Griffiths et al. 1998). Genomic studies of angiosarcomas have identified key driver mutations in genes linked to angiogenesis (Behjati et al. 2014). Truncating mutations in *PTPRB* (an endothelial phosphatase and negative regulator of vascular growth factor tyrosine kinases) and activating Arg707Gln missense mutations in *PLCG1* (a signal transducer of tyrosine kinase) have been reported (Behjati et al. 2014).

These mutations were not present in our case. Angiosarcoma is rarely seen in the context of XP; there are 11 reports of angiosarcoma in XP patients, with most of these ($n = 10$) occurring on the head and neck (Leake et al. 1992; De Silva et al. 1999; Ludolph-Hauser et al. 2000; Marcon et al. 2004; Arora et al. 2008; Olson et al. 2012; Sharma et al. 2012; Karkouche et al. 2013). Of these, seven patients were treated with surgical excision, three with surgery plus radiotherapy, and one with chemotherapy. Only two patients had local recurrence, and no metastatic disease was observed over a mean follow-up period of 1–40 months. Chemotherapy and radiotherapy can be used in patients with XP in most cases, but specialist advice is suggested. Anti-PD-L1 inhibition has been successfully used for the treatment of metastatic melanoma and metastatic cutaneous squamous cell carcinomas in patients with XP (Deinlein et al. 2017; Salomon et al. 2018).



Figure 5. Clinical images showing large soft tissue mass on left jaw that was causing tracheal compression (A) and post three cycles of pembrolizumab (B).

Angiosarcoma and Its Treatment

Cutaneous angiosarcoma is managed with surgical excision of the primary tumor, with or without postoperative radiotherapy. Chemotherapy with doxorubicin or paclitaxel has been used for metastatic disease, and based on data from retrospective and prospective trials, its true value is unclear. Sindhu et al. (2017) report a patient with metastatic angiosarcoma expressing PD-L1, treated with off-label pembrolizumab 2 mg/kg every 21 d for 13 cycles with shrinkage of his liver disease and no new facial lesions during an 8-mo follow-up period off treatment. To date, there are no immunotherapy agents licensed to treat angiosarcoma. Furthermore, secondary autoimmune-related complications have been reported with checkpoint inhibitor therapy. This is the first report of a patient with end-stage metastatic angiosarcoma on the background of XP being treated with immunotherapy.

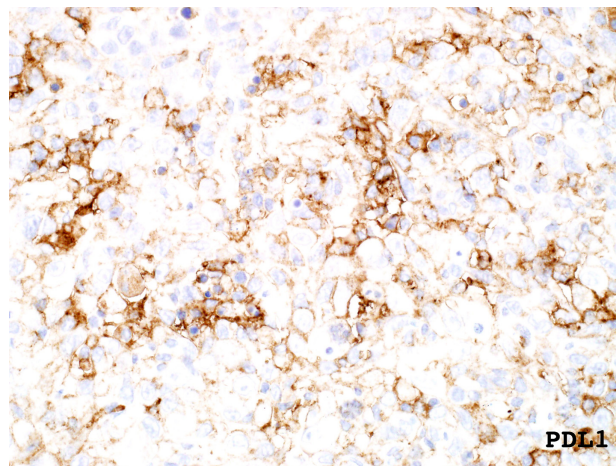


Figure 6. Immunohistochemistry performed on primary excision staining positive for PD-L1 (60%).

Table 1. Genomic analysis of the patient's primary angiosarcoma

Gene	Chromosome	Genomic location	HGVS DNA reference	HGVS protein reference	Variant type	Predicted effect	dbSNP/dbVar ID	Genotype
<i>POLE</i>	12	g.133249847G > A	c.1376C > T	p.S459F	Sub	Missense		Heterozygous
<i>TP53</i>	17	g.7578395 G > A	c.535C > T	p.H179Y	Sub	Missense	rs587780070	Heterozygous
<i>CDKN2A</i>	9	g. 21694602–23444942			Homozygous deletion	Whole gene deletion		Homozygous

CONCLUSION

In the last decade, whole-genome sequencing has enabled us to visualize every mutation present in a human cancer genome, allowing us to gain insights into the drivers and mutational signatures present in an individual's cancer. Mutational signatures can offer unique insights into the pathogenesis of a cancer and provide information that may be translated into possible therapeutic and preventative treatments (Nik-Zainal et al. 2016). In this case, mutational signatures from WGS have been used as a biomarker to guide immunotherapy. Our patient had none of the classical "drivers" seen in an angiosarcoma, possibly explaining why he progressed after three lines of "standard" treatment. The histological appearances were a poor predictor of treatment response, whereas the molecular fingerprint was an excellent predictor of response to therapy with pembrolizumab. We hope that as WGS becomes an integral part of cancer care, cancer treatments will be stratified to the individual based on their unique mutational makeup as opposed to the classical method of histological based treatment decisions. Because formal clinical trials are not possible in ultra-rare situations such as this one, mutational fingerprinting in individual cases and small patient cohorts will be critical in providing effective therapies to these patients.

METHODS

Immunohistochemistry

Immunohistochemistry was performed and positive for the vascular markers CD31 and ERG. Negative markers included S100, CD34, and MFT 116.

Table 2. Table showing quality control metrics for whole-genome sequencing

Sequence metrics	Sequencing method	Whole-genome sequencing
	Tumor coverage	35.6×
	Normal coverage	31.09×
	Additional text	Duplicate read rate < 10%
Processing	Alignment	BWA v2.0.54
	Substitutions	CaVEMan v1.11.2
	Indels	Pindel v2.2.2
	Rearrangements	Brass v5.4.1
	Copy number	ASCAT (NGS) v4.0.1
Raw data	Substitutions	805,261
	Indels	1007
	Rearrangements	11
Ploidy	1.85	
Aberrant cell fraction	0.35	

Genomic sequencing

WGS was performed on genomic DNA from the original tumor and peripheral blood lymphocytes, using Illumina HiSeq X TEN, 150-bp paired-end sequencing technology. Average tumor coverage was 35.6× and average normal coverage was 31.09× (Table 2). Short reads were aligned to build GRCh37 using BWA v2.0.54, substitutions called using CaVEMan v1.11.2, indels called using Pindel v2.2.2, structural variation called using Brass v5.4.1, and copy number using ASCAT (NGS) v4.0.1. Total ploidy was estimated to be 1.85.

ADDITIONAL INFORMATION

Data Deposition and Access

The raw sequencing data has been submitted to the European Genome-phenome Archive (EGA) (<https://ega-archive.org/>) under accession number EGAD00001004786. The variants have been uploaded to Mendeley and can be found under doi number: 10.17632/7cxt72pckw.1 (<https://data.mendeley.com/datasets/7cxt72pckw/1>).

Ethics Statement

The patient has consented for all aspects of his care to be published including clinical photography. WGS was performed as a part of a clinical research project and was approved by the U.K. National Research Ethics Service.

Acknowledgments

We thank Professor Alan Lehmann, University of Sussex, for an expert opinion on DNA repair and xeroderma pigmentosum, and Dr Robin Jones, Royal Marsden Hospital, London, for delivery of the clinical trial.

Funding

This work was funded by a Cancer Research UK (CRUK) Advanced Clinician Scientist Fellowship (C60100/A23916) and a Wellcome-Beit Prize.

Competing Interest Statement

S.N.-Z. is an inventor on four published patents and one additional patent application in review, none of which is relevant to the current manuscript.

Received May 22, 2019; accepted in revised form August 26, 2019.

REFERENCES

- Alexandrov LB, Nik-Zainal S, Wedge DC, Aparicio SAJR, Behjati S, Biankin AV, Bignell GR, Bolli N, Borg A, Børresen-Dale A-L, et al. 2013. Signatures of mutational processes in human cancer. *Nature* **500**: 415–421. doi:10.1038/nature12477
- Arora R, Sharma A, Gupta R, Vijayaraghavan M. 2008. Cutaneous angiosarcoma in a patient with xeroderma pigmentosum. *Indian J Pathol Microbiol* **51**: 504–506. doi:10.4103/0377-4929.43741
- Behjati S, Tarpey PS, Sheldon H, Martincorena I, Van Loo P, Gundem G, Wedge DC, Ramakrishna M, Cooke SL, Pillay N, et al. 2014. Recurrent *PTPRB* and *PLCG1* mutations in angiosarcoma. *Nat Genet* **46**: 376. doi:10.1038/ng.2921
- Bradford PT, Goldstein AM, Tamura D, Khan SG, Ueda T, Boyle J, Oh K-S, Imoto K, Inui H, Moriwaki S-I, et al. 2011. Cancer and neurologic degeneration in xeroderma pigmentosum: long term follow-up characterises the role of DNA repair. *J Med Genet* **48**: 168–176. doi:10.1136/jmg.2010.083022
- Brash DE. 2015. UV signature mutations. *Photochem Photobiol* **91**: 15–26. doi:10.1111/php.12377
- Cancer Genome Atlas Network. 2012. Comprehensive molecular characterization of human colon and rectal cancer. *Nature* **487**: 330–337. doi:10.1038/nature11252
- Deinlein T, Lax SF, Schwarz T, Giuffrida R, Schmid-Zalaudek K, Zalaudek I. 2017. Rapid response of metastatic cutaneous squamous cell carcinoma to pembrolizumab in a patient with xeroderma pigmentosum: case report and review of the literature. *Eur J Cancer* **83**: 99–102. doi:10.1016/j.ejca.2017.06.022
- De Silva BD, Nawroz I, Doherty VR. 1999. Angiosarcoma of the head and neck associated with xeroderma pigmentosum variant. *Br J Dermatol* **141**: 166–167. doi:10.1046/j.1365-2133.1999.02947.x

- Fasshi H, Sethi M, Fawcett H, Wing J, Chandler N, Mohammed S, Craythorne E, Morley AMS, Lim R, Turner S, et al. 2016. Deep phenotyping of 89 xeroderma pigmentosum patients reveals unexpected heterogeneity dependent on the precise molecular defect. *Proc Natl Acad Sci* **113**: E1236–E1245. doi:10.1073/pnas.1519444113
- Gargiulo P, Della Pepa C, Berardi S, Califano D, Scala S, Buonaguro L, Ciliberto G, Brauchli P, Pignata S. 2016. Tumor genotype and immune microenvironment in POLE-ultramutated and MSI-hypermutated endometrial cancers: new candidates for checkpoint blockade immunotherapy? *Cancer Treat Rev* **48**: 61–68. doi:10.1016/j.ctrv.2016.06.008
- Gentzler R, Hall R, Kunk PR, Gaughan E, Dillon P, Slingluff CL, Rahma OE. 2016. Beyond melanoma: inhibiting the PD-1/PD-L1 pathway in solid tumors. *Immunotherapy* **8**: 583–600. doi:10.2217/imt-2015-0029
- Griffiths CE, Barker JW, Bleiker T, Chalmers R, Creamer D. 1998. *Rook's textbook of dermatology*, 8th ed. Blackwell Scientific, Oxford.
- Howitt BE, Shukla SA, Sholl LM, Ritterhouse LL, Watkins JC, Rodig S, Stover E, Strickland KC, D'Andrea AD, Wu CJ, et al. 2015. Association of polymerase e-mutated and microsatellite-unstable endometrial cancers with neoantigen load, number of tumor-infiltrating lymphocytes, and expression of PD-1 and PD-L1. *JAMA Oncol* **1**: 1319–1323. doi:10.1001/jamaoncol.2015.2151
- Karkouche R, Kerob D, Battistella M, Soufir N, Hadj-Rabia S, Bagot M, Lebbé C, Bourrat E. 2013. Angiosarcoma in patients with xeroderma pigmentosum: less aggressive and not so rare? *J Am Acad Dermatol* **69**: e142–e143. doi:10.1016/j.jaad.2013.03.011
- Kleijer WJ, Laugel V, Berneburg M, Nardo T, Fawcett H, Gratchev A, Jaspers NGJ, Sarasin A, Stefanini M, Lehmann AR. 2008. Incidence of DNA repair deficiency disorders in western Europe: xeroderma pigmentosum, Cockayne syndrome and trichothiodystrophy. *DNA Repair (Amst)* **7**: 744–750. doi:10.1016/j.dnarep.2008.01.014
- Leake J, Sheehan MP, Rampling D, Ramani P, Atherton DJ. 1992. Angiosarcoma complicating xeroderma pigmentosum. *Histopathology* **21**: 179–181. doi:10.1111/j.1365-2559.1992.tb00370.x
- Ludolph-Hauser D, Thoma-Greber E, Sander C, Sommerhoff CP, Röcken M. 2000. Mast cells in an angiosarcoma complicating xeroderma pigmentosum in a 13-year-old girl. *J Am Acad Dermatol* **43**: 900–902. doi:10.1067/mjd.2000.101883
- Marcon I, Collini P, Casanova M, Meazza C, Ferrari A. 2004. Cutaneous angiosarcoma in a patient with xeroderma pigmentosum. *Pediatr Hematol Oncol* **21**: 23–26. doi:10.1080/08880010490263380
- Nik-Zainal S, Davies H, Staaf J, Ramakrishna M, Glodzik D, Zou X, Martincorena I, Alexandrov LB, Martin S, Wedge DC, et al. 2016. Landscape of somatic mutations in 560 breast cancer whole-genome sequences. *Nature* **534**: 47–54. doi:10.1038/nature17676
- Olson MT, Puttgen KB, Westra WH. 2012. Angiosarcoma arising from the tongue of an 11-year-old girl with xeroderma pigmentosum. *Head Neck Pathol* **6**: 255–257. doi:10.1007/s12105-011-0303-x
- Pleasance ED, Cheetham RK, Stephens PJ, McBride DJ, Humphray SJ, Greenman CD, Varela I, Lin M-L, Ordóñez GR, Bignell GR, et al. 2010. A comprehensive catalogue of somatic mutations from a human cancer genome. *Nature* **463**: 191–196. doi:10.1038/nature08658
- Salomon G, Maza A, Boulinguez S, Paul C, Lamant L, Tournier E, Mazereeuw-Hautier J, Meyer N. 2018. Efficacy of anti-programmed cell death-1 immunotherapy for skin carcinomas and melanoma metastases in a patient with xeroderma pigmentosum. *Br J Dermatol* **178**: 1199–1203. doi:10.1111/bjd.16270
- Sharma S, Deshmukh AD, Bal M, Chaukar DA, Dcruz AK. 2012. Angiosarcoma of the scalp associated with xeroderma pigmentosum. *Indian J Med Paediatr Oncol* **33**: 126–129. doi:10.4103/0971-5851.99753
- Shinbrot E, Henninger EE, Weinhold N, Covington KR, Göksenin AY, Schultz N, Chao H, Doddapaneni H, Muzny DM, Gibbs RA. 2014. Exonuclease mutations in DNA polymerase epsilon reveal replication strand specific mutation patterns and human origins of replication. *Genome Res* **24**: 1740–1750. doi:10.1101/gr.174789.114
- Sindhu S, Gimber LH, Cranmer L, McBride A, Kraft AS. 2017. Angiosarcoma treated successfully with anti-PD-1 therapy—a case report. *J Immunother Cancer* **5**: 58. doi:10.1186/s40425-017-0263-0



Dramatic response of metastatic cutaneous angiosarcoma to an immune checkpoint inhibitor in a patient with xeroderma pigmentosum: whole-genome sequencing aids treatment decision in end-stage disease

Sophie Momen, Hiva Fassihi, Helen R. Davies, et al.

Cold Spring Harb Mol Case Stud 2019, **5**: a004408

Access the most recent version at doi:[10.1101/mcs.a004408](https://doi.org/10.1101/mcs.a004408)

References This article cites 24 articles, 3 of which can be accessed free at:
<http://molecularcasestudies.cshlp.org/content/5/5/a004408.full.html#ref-list-1>

License This article is distributed under the terms of the Creative Commons Attribution License, which permits unrestricted reuse and redistribution provided that the original author and source are credited.

Email Alerting Service Receive free email alerts when new articles cite this article - sign up in the box at the top right corner of the article or [click here](#).
